

Observations of surf infrasound in Hawai‘i

M. Garcés, C. Hetzer, M. Merrifield, M. Willis, and J. Aucan

HIGP, SOEST, University of Hawai‘i at Mānoa, Hawai‘i, USA

Received 12 September 2003; accepted 6 November 2003; published 20 December 2003.

[1] Comparison of ocean buoy measurements with infrasonic array data collected during the epic winter of 2002–2003 shows a clear relationship between breaking ocean wave height and infrasonic signal levels. In addition, infrasonic arrays allow the identification of distinct breaking zones along the shoreline. Our observations suggest that infrasonic measurements can be used in conjunction with buoys to estimate wave heights, identify regions of high wave action, and validate surface wave propagation models. **INDEX TERMS:** 4560 Oceanography: Physical: Surface waves and tides (1255); 4594 Oceanography: Physical: Instruments and techniques; 4544 Oceanography: Physical: Internal and inertial waves; 0394 Atmospheric Composition and Structure: Instruments and techniques; 0350 Atmospheric Composition and Structure: Pressure, density, and temperature. **Citation:** Garcés, M., C. Hetzer, M. Merrifield, M. Willis, and J. Aucan, Observations of surf infrasound in Hawai‘i, *Geophys. Res. Lett.*, 30(24), 2264, doi:10.1029/2003GL018614, 2003.

1. Introduction

[2] Low frequency sound below the hearing threshold of the human ear is generated by large-scale processes that rapidly displace or compress substantial amounts of air [e.g., *Hedlin et al.*, 2002]. A breaking wave may generate infrasound by (1) violently collapsing against itself, as in the production of a tube, (2) slamming against a cliff or jetty, and (3) impacting against a shallow reef. Most work on surf acoustics has concentrated on high frequencies associated with bubble oscillations or low frequencies associated with microseisms [*Kerman*, 1988]. In this paper, we concentrate on the 1–5 Hz frequency range where most of the infrasonic energy associated with breaking surf appears to be concentrated.

2. Instrumentation

[3] Infrasound station I59US, Hawaii, is part of the global infrasound network of the International Monitoring System [*Vivas-Veloso et al.*, 2002]. Due to the station’s location leeward of the massive volcanoes and in a dense tropical forest, the Hawaii station has very low ambient noise levels and is one of the most sensitive stations of the IMS. The station consists of four Chaparral 5 microphones with a passband of 0.05–8 Hz and a dynamic range exceeding 120 dB. Three of the sensors are arranged as a triangle with a 2 km baseline, with the fourth sensor near the center of the triangle. Sensor data is recorded by 24-bit digitizers and sent in real time via radio telemetry to the Infrasound Laboratory in Keahole Point, West Hawaii.

[4] The portable data acquisition system we used to collect nearshore data is described in *Garcés et al.* [2003]. It consists of a six-channel Geotech DL 24-bit digitizer recording at 100 sps. Two of the channels acquire wind speed and direction, and the remaining channels collect data from a four-element infrasonic array deployed as a triangle with a central element. The sensors have -3 dB points at 0.9 Hz and 20 Hz, with a peak sensitivity of 150 mV/Pa at 5 Hz. During a temporary deployment in West Hawaii from January 9–14, 2003, we used a 4-element triangular array with a central element and an aperture of ~ 100 m. We applied the PMCC algorithm of *Cansi* [1995] to detect coherent infrasonic energy across the array and extract the speed, arrival angle, and amplitude of the detected arrivals.

[5] The Waimea Bay wave buoy is a Datawell directional waverider buoy that has been deployed since December 2001 and is located 6.5 km WNW of Waimea Bay, Oahu. The buoy measures horizontal and vertical accelerations, and calculates a full frequency/direction wave spectrum every 30 minutes [*Longuet-Higgins et al.*, 1963].

3. Features of Surf Infrasound

[6] Typical infrasonic signals associated with large surf are shown in Figure 1 for a portable array deployed ~ 200 m from the shoreline and for I59US, with a range of ~ 7.5 km from the nearest shore. Figure 2 shows a spectrogram in the 0.6–6 Hz band for a single channel of infrasound array I59US over the period of January 1–29, 2003. Superposed

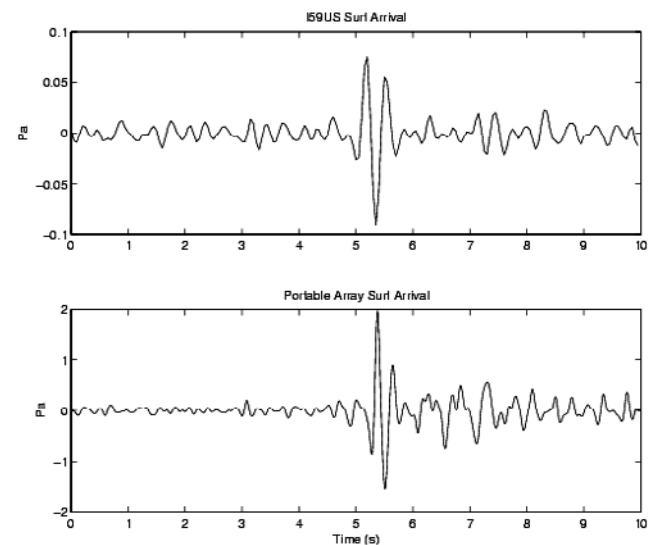


Figure 1. Typical waveforms for surf-associated events recorded ~ 200 m from the coast (upper panel) and ~ 7.5 km from the coast (lower panel).

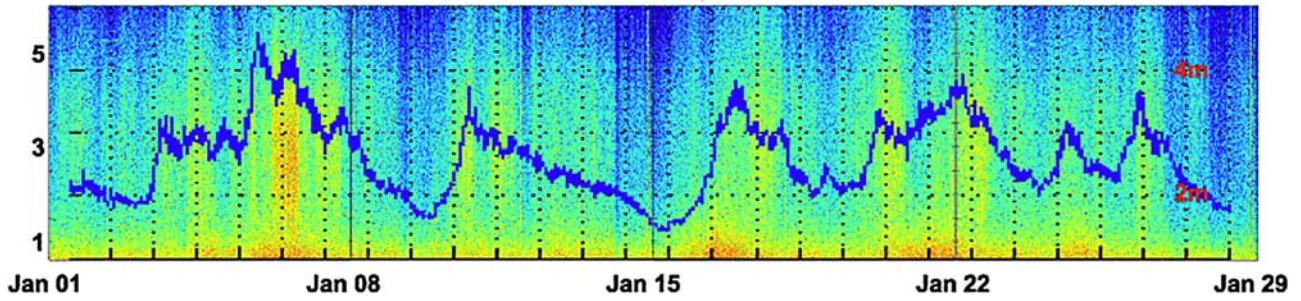


Figure 2. Overlay of ocean wave height from the Waimea buoy (blue) over the spectrogram for one channel of I59US during the month of January 2003. The red tick marks denote GMT time for the acoustic data, the scale for the wave height is on the right hand side, and the vertical axis on the left hand side is infrasonic frequency, in hertz.

over the spectrogram is a plot of the wave height observed at the Waimea buoy. The Waimea buoy data has been time shifted to allow for the propagation delay from Waimea, Oahu to Kona, West Hawaii. The buoy was located at 21.6733°N 158.1167°W, at a range of 326 km and a bearing of 315.2 degrees from I59US. Thus, depending on the dominant period (10–18 s), a NW swell would take between 7 to 10 hours to arrive on Hawaii. There is clear correlation between the ocean wave height and the infrasonic energy in the 1–5 Hz frequency band. However, one obvious discrepancy is that the swells of January 5 and January 10 were not observed in Kona. This discrepancy can be easily explained by the different exposure angle of the Waimea buoy and the high dependence on swell direction of the surf observed on the Western side of the Big Island of Hawaii (Figure 3). A numerical coastal wave model was used to visualize the swell patterns in the lee of the Islands. The coastal model was initialized at the domain

boundaries with the output spectrum from the global Wave-watch III wave model for January 10, 2003, using a period of 17 s and a significant wave height of 6 meters arriving from 320°. As shown in Figure 3, the Hawaii chain shadows NNW swells from reaching the Kona coast, explaining why such swells are not observed acoustically.

[7] A single breaking wave front may generate multiple pressure pulses as it collapses into multiple sections or interacts with different segments of the reef or adjacent cliffs. However, each of these pulses will have a different arrival direction, thus permitting the identification of specific regions of wave action. If the array is relatively far from the coast, then the observed infrasonic field provides a measure of the swell energy distribution along a large portion of the shoreline. However, if an array is close to

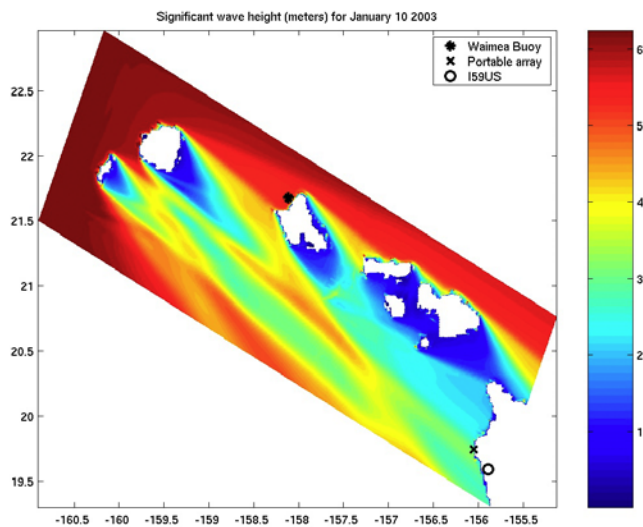


Figure 3. Island shadow map for a typical NW winter swell. The location of the Waimea buoy, I59US, and the portable array are shown in the figure. The color bar shows significant wave height in meters. For this swell direction, the western coast of the island of Hawaii is heavily shadowed by the island chain.

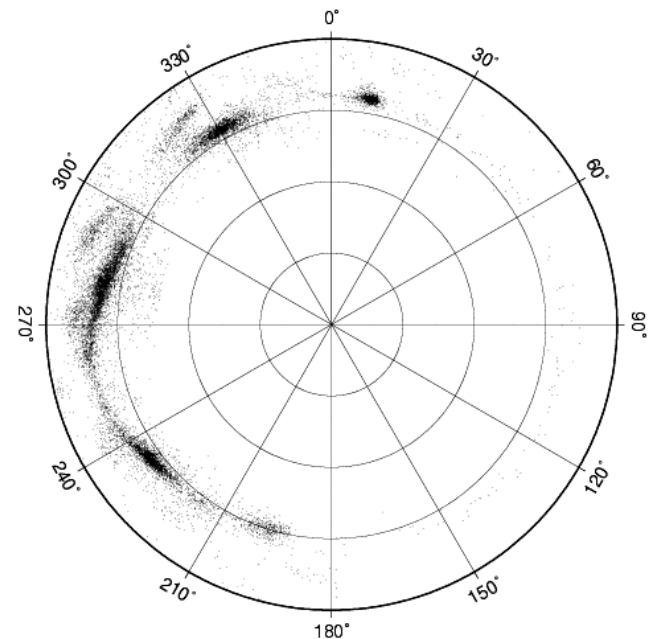


Figure 4. Azimuth plot showing the distribution of arrival angles for surf events during January 10–14 at a portable array ~200 m from the shore. Distinct areas of wave action can be identified. The radial distance denotes apparent horizontal wave slowness in 100 s/degree intervals.

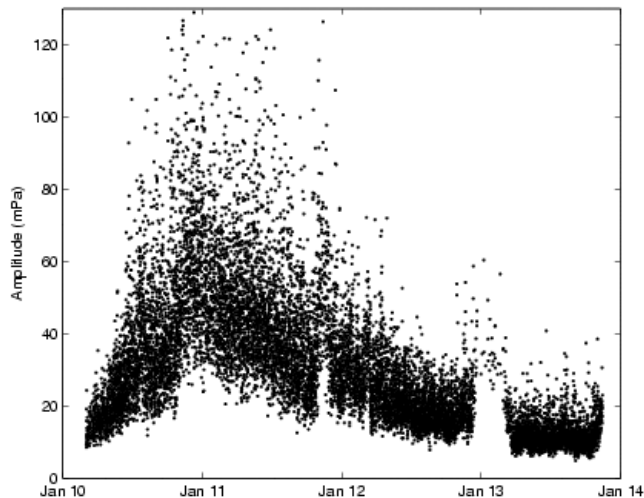


Figure 5. Infrasonic amplitude (in millipascals) for the January 10–14 swell. The rate of growth and decay observed in the acoustic amplitudes for this swell roughly match those observed in the wave buoy data. The gaps in the detections correspond to periods of high wind noise.

the shore, it is possible to identify distinct regions of wave action (Figure 4). Infrasonic arriving at the portable near-shore array from an azimuth of 330 and 10 degrees appeared concentrated in a narrow beam, whereas arrivals from 260–300 degrees and 220–240 degrees appeared to have a broader spatial distribution. Further studies are needed to relate the sound directivity to swell direction, bathymetry, and wave breaking dynamics. However, a clear relationship between ocean wave height and infrasonic amplitude can be observed in Figures 2 and 5, where the rates of growth and decay observed in the infrasonic data roughly matches those of the ocean buoy observations.

[8] We note that littoral signals may also be observed at I59US even when there are no significant swells in the area.

These signals may be associated with waves trapped in bays, and will be discussed in a separate manuscript.

4. Concluding Remarks

[9] Large surf can generate infrasonic signals in the 1–5 Hz frequency band. The amplitude of the infrasonic is proportional to the ocean wave height and may permit detailed estimates of how ocean waves interact with the coastline. Acoustic arrays also provide directional information that may be used for quantifying wave action at specific locations. Integration of ocean buoys with land-based infrasonic stations may facilitate the testing and validation of global and near shore mesoscale ocean wave propagation models.

[10] **Acknowledgments.** This work has been funded by Defense Threat Reduction Agency contracts DTRA01-00-C-0106 and DTRA01-01-C-0077. This is HIGP# 1313, SOEST# 6295.

References

- Cansi, Y., An automatic seismic event processing for detection and location: The P. M. C. C. method, *Geophys. Res. Lett.*, 22, 1021–1024, 1995.
- Garcés, M., A. Harris, C. Hetzer, J. Johnson, S. Rowland, E. Marchetti, and P. Okubo, Infrasonic tremor observed at Kilauea Volcano, Hawaii, *Geophys. Res. Lett.*, 30(20), 2023, doi:10.1029/2003GL018038, 2003.
- Hedlin, M., M. Garcés, H. Bass, C. Hayward, E. Herrin, J. Olson, and C. Wilson, Listening to the secret sounds of Earth's atmosphere, *Eos Trans. AGU*, 83(557), 564–565, 2002.
- Kerman, B. R., *Sea Surface Sound*, Kluger Academic Publishers, Dordrecht, 1988.
- Longuet-Higgins, M. S., D. E. Cartwright, and N. D. Smith, Observations of the directional spectrum of sea waves using the motion of a floating buoy, in *Ocean Wave Spectra*, Prentice-Hall, Englewoods Cliffs, NJ, 111–136, 1963.
- Vivas-Veloso, J., D. Christie, T. Hoffmann, E. Demirovic, P. Campus, M. Bell, A. Molero, A. Langlois, P. Martysevich, J. Carvalho, and A. Kramer, Status of the IMS Infrasonic Network, paper presented at the Infrasonic Technology Workshop, De Bilt, Netherlands, October 28–31, 2002.

J. Aucan, M. Garcés, C. Hetzer, M. Merrifield, and M. Willis, HIGP, SOEST, University of Hawai'i at Mānoa, Hawai'i, USA. (milton@isla.hawaii.edu)